

# High Performance Substrate Integrated Waveguide Bandstop Filter using Dual-radial Cavity Resonator

G. S. Tan, M. N. Husain, K. S. Tan  
Department of Telecommunication Engineering  
Faculty of Electronic and Computer Engineering (FKEKK)  
Universiti Teknikal Malaysia Melaka (UTeM), Malaysia  
gansiang@student.utem.edu.my

**Abstract**— A SIW bandstop filter is designed by coupling two cavity resonators to the SIW line. Dual-radial cavity resonators are proposed to design the SIW bandstop filter. Two single radial cavity resonator SIW bandstop filter are designed first. After that, a dual-radial cavity resonator SIW bandstop filter is designed based on the two single radial cavity resonator SIW bandstop filter. The designed bandstop filter operates at X-band frequency with a stopband from 8.7GHz to 9.2GHz, and it is implemented on RO4350B substrate with a thickness of 0.508mm. An insertion loss of less than 3dB is achieved, and the bandstop filter have a sharp roll off with attenuation of -34dB. This bandstop filter can be applied in the radar system.

**Index Terms**—Bandstop Filter, Substrate Integrated Waveguide, Cavity Resonator, Stopband Bandwidth

## I. INTRODUCTION

Substrate Integrated Waveguide is constructed by two periodic rows of metallic via holes on a dielectric substrate [1]. It has the advantages of low loss, high quality factor and complete shielding. Filters are the most popular device among the passive SIW components. A SIW bandpass filter was etched with a complementary split-ring resonators on the SIW surface to achieve miniaturization [2]. A bandpass filter is developed using quater substrate integrated waveguide resonator loaded with a fractal-shaped [3]. A SIW dual-mode bandpass filter is etched with series of cross-slot structures to obtain miniaturization [4]. The two researches on Non-Bragg resonance in substrate integrated waveguide show that band rejection response is obtained with the design [5-6].

Several papers regarding the SIW bandstop filter that highlight techniques to design the SIW bandstop filter have been presented. For multiple bandstop filter, the proposed transversal coupling network is used in the design [7]. Single bandstop filters are designed with techniques, such as coupling cavity resonator to a strip line [8]; coupling stub SIW stripline resonator to the main SIW stripline [9]; directly connected two-stage branch couple to the two-port network SIW bandpass filter [10]; and even-odd-mode predistortion technique [11]. A coupling network was introduced for a dual-band SIW bandstop filter design [12].

Rectangular cavity resonator is a common structure that had been used in previous designs. In this paper, a radial cavity resonator is proposed to design a SIW bandstop filter. The

bandstop filter is designed by coupling the radial cavity resonator to the SIW line. The SIW line functions as the transmission line to transmit input signal to the load.

## II. SUBSTRATE INTEGRATED WAVEGUIDE BANDSTOP FILTER DESIGN

The SIW bandstop filter design starts with the design of the SIW line, followed by the radial cavity resonator design.

### A. Substrate Integrated Waveguide Transmission Line Design

From the research on the SIW structure, it shows that only  $TE_{M0}$  modes can be excited and extracted in the structure; therefore, TM modes do not exist in the SIW structure [13]. A research on the SIW line has suggested an equation of the resonant frequency  $f_c$  [14] as follow:

$$f_{c(TE10)} = \frac{c}{2\sqrt{\epsilon_r}} \left( W - \frac{d^2}{0.95 \cdot p} \right)^{-1} \quad (1)$$

$$W_{eff} = W - \frac{d^2}{0.95 \cdot p} \quad (2)$$

where  $W$  is the width of the SIW line,  $d$  is the diameter of the metallic via holes and  $p$  is the spacing between the via holes.

Several papers had investigated on the SIW and highlighted a set of design rules related to the diameter  $d$  and the spacing between the via holes  $p$  [14-16] as follows:

$$d < p < 2d \quad (3)$$

$$d < \lambda_g / 5 \quad (4)$$

$$p / \lambda_c < 0.25 \quad (5)$$

where  $\lambda_c$  is the cutoff wavelength, and  $\lambda_g$  is the guide wavelength.

The bandstop filter is designed to operate at 9GHz centre stopband frequency. By following the SIW equation as above and with optimization through the CST microwave studio simulation tool, a good response along the passband is obtained. This results in the resonant frequency of 6GHz and the  $W_{eff}$  length of 13.06mm. In order to minimize the loss that occurs in the SIW line, the length of the SIW line will be kept at the shortest length for the dual-radial cavity resonators to operate optimally [17].

**B. Coupling of the cavity resonator to SIW lines**

The radial cavity resonator is directly coupled to the SIW line. Through the optimization by tuning the cavity resonator placement, the position of the resonator that produces good bandstop response is at 20.19mm from the input of the SIW line to the centre of the cavity resonator. The input width of the cavity resonator which provides the connection between the resonator and SIW line is set at 8.3mm for the bandstop filter design.

**C. Configuration of the radial cavity resonator**

The configuration of the radial cavity resonator consists of three parameters which are the span degree, the radius and the coupling length represented by  $d_r$ ,  $r$  and  $l$  respectively. Figure 1 shows the configuration of the radial cavity resonator SIW bandstop filter.

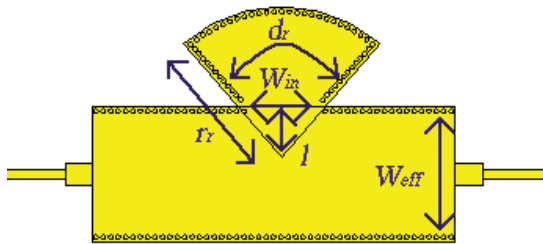


Figure 1: Configuration of the radial cavity resonator SIW bandstop filter

**III. SIMULATION RESULTS**

**A. Parametric study of the radial cavity resonator**

Parametric study on the radial cavity resonator is carried out to investigate the performance of the resonator by each parameter. The simulations are done by varying the value of one parameter while the rest of the dimensions are being kept constant.

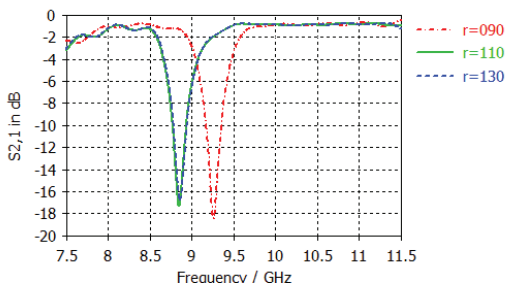


Figure 2: Frequency response of variation of degree of radial cavity resonator

degree of radial cavity resonator at 90°, 110° and 130°. Table 1 shows the centre stopband frequency, stopband bandwidth, attenuation and average insertion loss of the variation of degree of radial cavity resonator at 90°, 110° and 130°. From the results, it is observed that the increase in the parameter  $d_r$  will produce a bandstop response at a lower stopband frequency and narrower stopband bandwidth due to the change in the capacitor and inductor value in the resonator.

Table 1  
Results of variation of degree of radial cavity resonator

Degree $d_r$ (°)	Centre Stopband Frequency (GHz)	Stopband Bandwidth (MHz)	Attenuation (dB)	Average insertion loss (dB)
90	9.26	507	-18.5	-1.3
110	8.85	502	-17.4	-1.4
130	8.85	490	-16.9	-1.4

Figure 3 shows the frequency response of the variation of radius of radial cavity resonator at 14.7mm, 15.2mm and 15.7mm. Table 2 shows the centre stopband frequency, stopband bandwidth, attenuation and average insertion loss of the variation of degree of radial cavity resonator at 14.7mm, 15.2mm and 15.7mm. From the results, it is observed that the increase in the parameter  $r_r$  will produce a bandstop response at a lower stopband frequency and narrower stopband bandwidth due to the change in the capacitor and inductor value in the resonator.

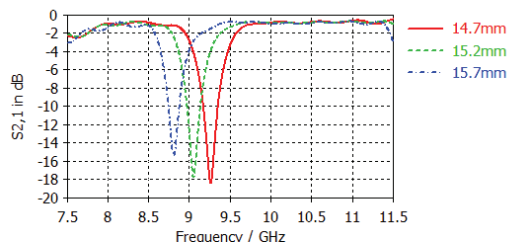


Figure 3: Frequency response of variation of radius of radial cavity resonator

Table 2  
Results of variation of radius of radial cavity resonator

Radius $r_r$ (mm)	Centre Stopband Frequency (GHz)	Stopband Bandwidth (MHz)	Attenuation (dB)	Average insertion loss (dB)
14.7	9.26	507	-18.5	-1.3
15.2	9.09	459	-17.2	-1.3
15.7	8.80	425	-15.4	-1.3

Figure 4 shows the frequency response of the variation of length of radial cavity resonator at 6mm, 5.5mm and 5mm. Table 3 shows the centre stopband frequency, stopband bandwidth, attenuation and average insertion loss of the variation of length of radial cavity resonator at 6mm, 5.5mm and 5mm. From the results, it is observed that the decrease in the parameter  $l$  will produce a bandstop response with a lower

attenuation level and narrower stopband bandwidth as the electric coupling and magnetic coupling both degenerate.

From the investigation, the parameter  $r$ , is the most crucial parameter in the radial cavity resonator since it has the most influence in the centre stopband frequency and stopband bandwidth. The parameter  $d$  has more effect on the centre stopband frequency, while the parameter  $l$  has more effect on the stopband bandwidth and attenuation.

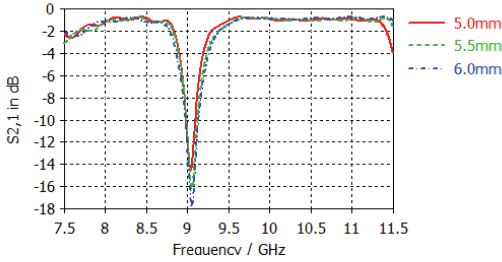


Figure 4: Frequency response of variation of length of radial cavity resonator

Table 3  
Results of variation of length of radial cavity resonator

Length / (mm)	Centre Stopband Frequency (GHz)	Stopband Bandwidth (MHz)	Attenuation (dB)	Average insertion loss (dB)
6	9.26	507	-18.5	-1.3
5.5	9.23	464	-17.7	-1.3
5	9.23	402	-16.3	-1.3

**B. Dual-radial cavity resonator bandstop filter**

From the simulation results of the single radial cavity resonator, the attenuation of the bandstop response is limited. The adding of second radial cavity resonator operates at the same frequency can increase the attenuation and selectivity of the bandstop filter. First, the parameters of the radial cavity resonator are simulated to give the bandstop response at 9GHz. In order to get a more precise result for the bandstop filter in measurement, the dielectric permittivity value for RO4350B is set to 3.66 for the simulation [18]. The resulted parameters for  $r1$  and  $r2$  are 14.7mm,  $d1$  and  $d2$  are  $90^\circ$  and  $l$  at 6mm. The position of the radial cavity resonators is tuned by length  $s11$  and  $s12$  to obtain an optimum bandstop response. The resulted length of  $s11$  and  $s12$  are 5.73mm and 33.45mm respectively. Figure 5 and Figure 6 show the configuration of the single radial cavity resonator at the length  $s11$  and length  $s12$ . The frequency response of the two single cavity resonator bandstop filter is shown in Figure 7 and Figure 8.

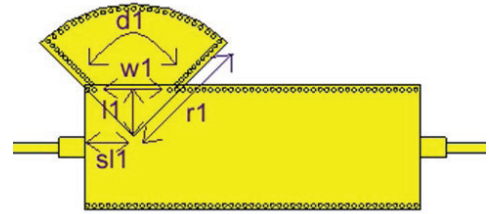


Figure 5: Configuration of single radial cavity resonator SIW bandstop filter at  $s11$

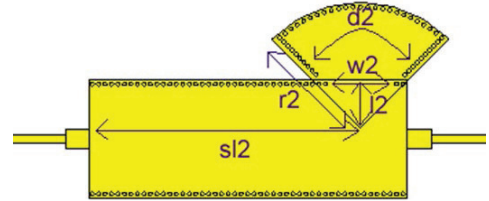


Figure 6: Configuration of single radial cavity resonator SIW bandstop filter at  $s12$

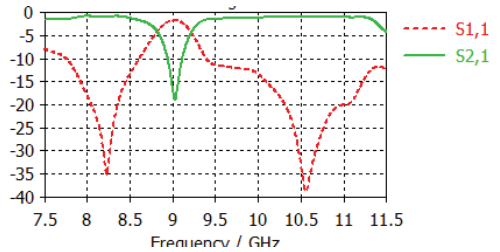


Figure 7: Frequency response of single radial cavity resonator SIW bandstop filter at  $s11$

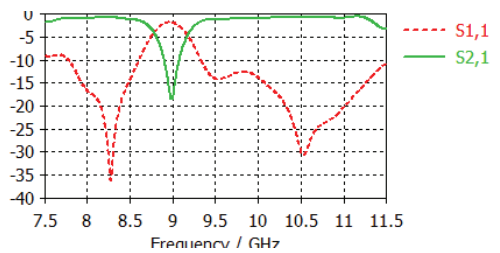


Figure 8: Frequency response of single radial cavity resonator SIW bandstop filter at  $s12$

Since the single radial cavity resonator bandstop filters with the length of  $s11$  and  $s12$  are obtained, a dual-radial cavity resonator can be formed by coupling two radial cavity resonators on a SIW line. Figure 9 shows the configuration of the dual-radial cavity resonator SIW bandstop filter. The frequency response of the dual-radial cavity resonator

bandstop filter is shown in Figure 10.

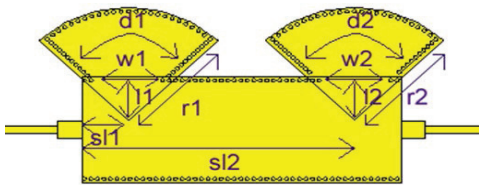


Figure 9: Configuration of dual-radial cavity resonator SIW bandstop filter

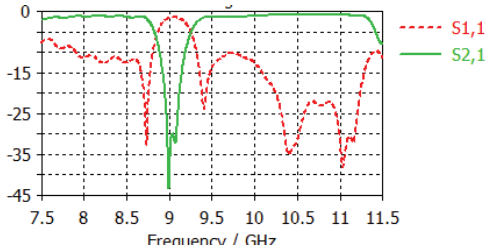


Figure 10: Frequency response of dual-radial cavity resonator SIW bandstop filter

Figure 10 shows that the coupling of the two radial cavity resonators on the SIW line have effectively increased the attenuation level of the bandstop filter. The dual-radial cavity resonator SIW bandstop filter has a sharp roll-off bandstop response.

### C. Measurement Results

The two single radial cavity resonator and dual-radial cavity resonator SIW bandstop filters are fabricated on RO4350B substrate using the standard PCB process to verify the simulation results. The substrate has a relative permittivity constant of 3.48 with 0.5mm thickness and has a loss tangent of 0.0037. The diameter of the via holes and the separation of the edge of the via holes are 0.5mm and 0.3mm respectively. Figure 11, Figure 12 and Figure 13 show the fabricated radial cavity resonator SIW bandstop filters.

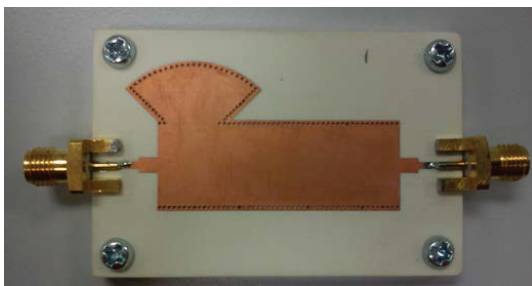


Figure 11: Fabricated single cavity resonator SIW bandstop filter at  $s11$

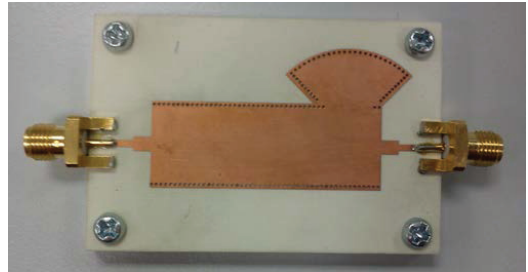


Figure 12: Fabricated single cavity resonator SIW bandstop filter at  $s12$

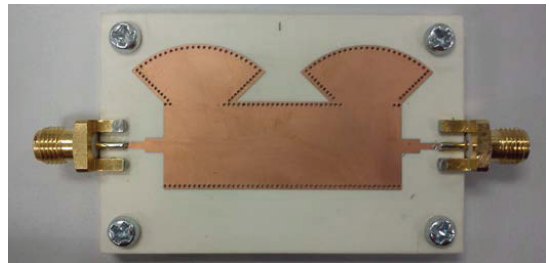


Figure 13: Fabricated dual-radial cavity resonator SIW bandstop filter

The measured frequency response for the radial cavity resonator SIW bandstop filters is shown in Figure 14, Figure 15 and Figure 16. The measured frequency responses show that there is only about 30MHz shift in the centre stopband frequency between the simulated and measured results. The measured average insertion loss of the bandstop filters is -3.4dB. The measured attenuation level for the dual-radial cavity resonator is about 34dB. Although losses occur in the dual-radial bandstop filter, the losses are acceptable as it is only slightly more than 3dB.

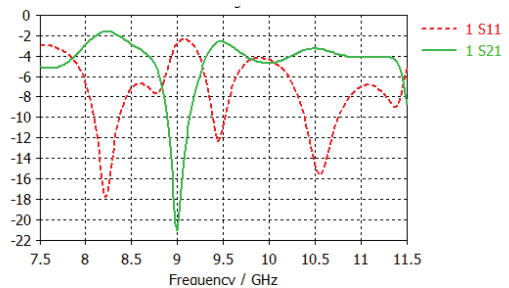


Figure 14: Frequency response of single cavity resonator SIW bandstop filter at  $s11$

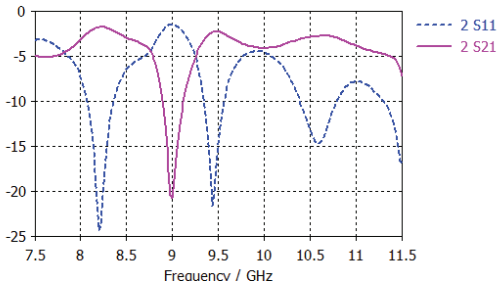


Figure 15: Frequency response of single cavity resonator SIW bandstop filter at  $s/2$

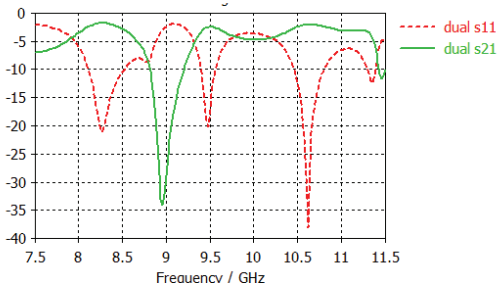


Figure 16: Frequency response of dual-radial cavity resonator SIW bandstop filter

IV. CONCLUSION

In this paper, the proposed radial cavity resonator is used to design a single and dual radial cavity resonator SIW bandstop filter. The radial cavity resonator is able to produce high performance bandstop response. The addition of another radial cavity resonator that operates at the same frequency has effectively improved the bandstop response. Through the optimization of the three parameters of the radial cavity resonator, the dual-radial cavity resonator SIW bandstop filter has achieved a high attenuation rate and sharp rejection level.

ACKNOWLEDGMENT

I would like to thank UTeM and Exploratory Research Grant Scheme for the sponsorship.

REFERENCES

- [1] Y. Cassivi, L. Perregrini, P. Arcioni, M. Bressan, K. Wu, and G. Conciauro, "Dispersion Characteristics of Substrate Integrated Rectangular Waveguide." *IEEE Microwave and Wireless Components Letters*, vol. 12, no.9, September 2002, pp.333-335.
- [2] Dong Y. D., Yang T. and Itoh T., "Substrate Intergrated Waveguide Loaded by complementary Split-ring Resonators and Its Applications to Miniaturized waveguide Filters." *Microwave Theory and Techniques*, *IEEE Transactions*, 57(9), 2211-2223.
- [3] Zhang, S., Bian, T. J., Zhai, Y., & Ren, Z. H., "Novel fractal-shaped bandpass filter using quarter substrate integrated waveguide resonator (QSIWR)." In *Microwave, Antenna, Propagation, and EMC Technologies for Wireless Communications (MAPE), 2011 IEEE 4th International Symposium on* (pp. 171-174). IEEE.
- [4] Chen, L. N., Jiao, Y. C., Zhang, Z., & Zhang, F. S., "Miniaturized substrate integrated waveguide dual-mode filters loaded by a series of cross-slot structures." *Progress In Electromagnetics Research C*, 29.
- [5] Cheng, X., Senior, D. E., Jao, P., Kim, J., Whalen, J. J., & Yoon, Y. K., "Non-Bragg resonance in substrate integrated waveguide." In *Antennas and Propagation Society International Symposium (APSURSI), 2010 IEEE* (pp. 1-4). IEEE.
- [6] Cheng, X., Kim, J., Kim, C., Jao, P., Senior, D. E., & Yoon, Y. K., "Corrugated substrate integrated waveguide with dual band non-Bragg resonance." In *Microwave Symposium Digest (MTT), 2011 IEEE MTT-S International* (pp. 1-4). IEEE.
- [7] Han S.H., Wang X.L., Fan Y., "Analysis and Design of Multiple-Band Bandstop Filters," *Progress in Electromagnetics Research*, PIER 70,297 - 306,
- [8] Badrul Hisham Ahmad and Ian. C. Hunter, "Design and Fabrication of a Substrate Integrated Waveguide Bandstop Filter," *Proc. of the 38th European Microwave Conference Amsterdam*. 40-42 2008
- [9] Badrul Hisham Ahmad, Ian c. Hunter, "Substrate Integrated Waveguide Bandstop Filter," *Journal of Telecommunication, Electronic and Computer Engineering*, Vol 2, No. 1, June 2010
- [10] Badrul Hisham, Ahmad, M. N. Husain, and K. S. Tan, "A Novel Hybrid Notch (HN) Substrate Integrated Waveguide (SIW) Bandstop Filter," *Journal of Telecommunication, Electronic and Computer Engineering (JTEC)*, UTeM 2.2 (2010): 13-17.
- [11] Zakaria, Zahrladha, and Ian Hunter, "Substrate Integrated Waveguide Filters based on even-and odd-mode Predistortion Technique," *Journal of Telecommunication, Electronic and Computer Engineering (JTEC)*, UTeM (2011): 61-71.
- [12] Yang, F., Yu, H. X., He, X. Y., Zhou, Y., & Liu, R. Z. "Novel multi-band filter design and Substrate Integrated Waveguide filter realization," In *Microwave Symposium Digest (MTT), 2012 IEEE MTT-S International* (pp. 1-3). IEEE.
- [13] F. Xu, K. Wu, "Guided-Wave and Leakage Characteristics of Substrate Integrated Waveguide," *IEEE Transactions on Microwave Theory and Techniques*, Vol. 53, NO 1, 66-73, January 2005.
- [14] D. Deslandes, K. Wu, "Accurate modeling, Wave Mechanisms, and Design Consideration of a Substrate Integrated Waveguide." *IEEE Trans. on Microwave Theory and Techniques*, 2006, vol. 54, no. 6, pp. 2516-2526.
- [15] F. Xu, K. Wu, "Guided-Wave and Leakage Characteristics of Substrate Integrated Waveguide," *IEEE Transactions on Microwave Theory and Techniques*, Vol. 53, NO 1, 66-73, January 2005.
- [16] K. Wu, Dominic Deslandes, and Yves Cassivi, "The Substrate Integrated Circuits - A New Concept for High-Frequency Electronic and Optoelectronics," *TELSIKS 2003*, October 1-3,2003.
- [17] Bozzi, M., Perregrini, L., Wu, K., & Arcioni, P. (2009). *Current and Future Research Trends in Substrate Integrated Waveguide Technology. Radioengineering*, 18(2).
- [18] Horn III, A. F., LaFrance, P. A., Reynolds, J. W., & Coonrod, J., "The influence of test method, conductor profile and substrate anisotropy on the permittivity values required for accurate modeling of high frequency planar circuits." *Circuit World*, 38(4), 219-231.

